Fuel Processing Technology 256 (2024) 108065

Contents lists available at ScienceDirect

Fuel Processing Technology

journal homepage: www.elsevier.com/locate/fuproc

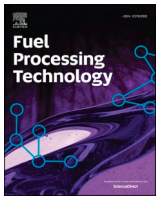

Uncovering the potential of MSC CT-350 for CO_2/CH_4 separation toward the optimization of a Pressure Swing Adsorption process for biogas upgrading

Esther Pancione [a], Francesco La Motta [b], Alessandro Boffa [b], Amedeo Lancia [a], Alessandro Erto [a,*]

[a] Dipartimento di Ingegneria Chimica, dei Materiali e della Produzione Industriale, Università degli Studi di Napoli Federico II, Piazzale Vincenzo Tecchio 80, 80125 Napoli, Italy
[b] OILTECH srl, Via Caviglia, 3, 20139 Milano, Italy

ARTICLE INFO

Keywords:
Biogas upgrading
Carbon molecular sieve
Breakthrough curve
Adsorbent regeneration
Pressure swing adsorption

ABSTRACT

A laboratory-scale fixed-bed column is employed to study the dynamic behavior of the carbon molecular sieve MSC CT-350 for CO_2/CH_4 separation. Breakthrough adsorption tests in single-component systems are carried out at different pressures (1, 3, 5, 6.5 and 8 bar) and constant temperature (20 °C). Moreover, an additional test is conducted with a 40% CO_2/60% CH_4 binary mixture at 3 bar. Desorption tests are performed by varying the purge-to-feed ratio (P/F) at 50%, 30% and 20%, optionally using a vacuum pump. Experimental results show that MSC CT-350 has a good CO_2 adsorption capacity for each pressure, considerably higher than CH_4. In the binary test, very slight differences are experimentally found in the adsorption kinetics and equilibrium adsorption capacity with respect to single-compound tests, which results equal to 2.16 mol kg^{-1} for CO_2 and 0.302 mol kg^{-1} for CH_4 at 3 bar, compared with 2.29 mol kg^{-1} for CO_2 and 0.262 mol kg^{-1} for CH_4 for the single-compoound counterparts. The time required for a complete regeneration decreases with the increase in purge flowrate and with the simultaneous use of the vacuum pump. Finally, CO_2 adsorption is a reversible process as the CO_2 adsorption capacity of the adsorbent is not significantly reduced when utilized in subsequent adsorption-desorption cycles.

1. Introduction

The continue development of society and increasing energy demands have resulted in the over-exploitation of fossil fuels, which has determined a huge growth of greenhouse gas (GHG) emissions. In turn, this has contributed to global warming, highlighting the urgent need to explore new and sustainable energy sources. The current worldwide share of renewable energy is only approximately 16% of the total [1]. This highlights the necessity for creating plans to improve energy efficiency, lower net CO_2 emissions, and enhance renewable energy sources. Biogas derived from anaerobic digestion has the potential to be a viable and sustainable alternative, as it allows generating energy from waste and reducing the need for fossil fuels. Furthermore, biomethane produced from biogas by purification and upgrading processes (i.e. through CO_2 removal) can replace natural gas in existing infrastructure, such as pipelines and vehicles, without needing any modifications [2]. The revised Renewable Energy Directive has set a new binding target for the EU for 2030, which should reach at least 42.5% of renewable energy, higher than the previous 32% target [3]. The obvious environmental and economic benefits of biomethane have led to a significant increase in the number of biogas upgrading plants in Europe, from 483 to 729 in the period 2018 to 2020 [4].

Currently, among the available biogas upgrading technologies, adsorption processes are frequently preferred due to their efficiency, separation performance, and versatility [5].

During adsorption operations, the raw biogas stream to be purified flows through a column containing a fixed bed of porous material, which selectively retains the CO_2 molecules, enriching the methane content of the gaseous outlet stream. When the adsorbent material becomes saturated, to favor the desorption process, techniques such as Pressure Swing Adsorption (PSA) or Vacuum Swing Adsorption (VSA) can be used. PSA uses higher than atmospheric pressure during the adsorption step and

* Corresponding author.
E-mail addresses: esther.pancione@unina.it (E. Pancione), f.lamotta@oiltech.it (F. La Motta), a.boffa@oiltech.it (A. Boffa), amedeo.lancia@unina.it (A. Lancia), aleserto@unina.it (A. Erto).

https://doi.org/10.1016/j.fuproc.2024.108065
Received 12 January 2024; Received in revised form 19 February 2024; Accepted 22 February 2024
Available online 1 March 2024

maintains atmospheric pressure during the desorption step, whereas VSA uses atmospheric pressure for adsorption and sub-atmospheric pressure for desorption. These two technologies can be combined in the Vacuum Pressure Swing Adsorption (VPSA) cycle. In this case, adsorption usually takes place at a pressure of 4–10 bar, while desorption is done with a vacuum pump at a pressure of 0.1–0.2 bar [6].

The PSA separation process involves alternating adsorption and desorption steps in the column (swing adsorption). After proper conditioning, the final result is a stream that is significantly higher in CH_4 concentration (> 97% *v/v*) and may be comparable to the natural gas (NG) supply stream [7]. The PSA processes are cyclic in nature (adsorption-desorption) and typically require the use of multiple columns for a continuous production, accomplished through a series of interacting steps [8].

The choice of the adsorbent is crucial to ensure a high process efficiency and requires appropriate characteristics in terms of adsorption capacity and selectivity [9].

Most of the commercially available adsorbents used for CO_2 separation are physical adsorbents, primarily due to the low energy penalty for regeneration. Carbon-based materials have significant advantages, such as low cost, versatility, and the possibility to be produced and synthesized from a wide range of natural carbon-based materials. In particular, carbon molecular sieves (CMS) have played a pivotal role in the successful development and commercialization of gas separation units using PSA technology. These sieves feature uniform micropore diameters that allow the penetration of carbon dioxide while restricting the diffusion of methane molecules, thereby achieving a high selectivity toward CO_2 compared with CH_4 [10–12].

Preliminary dynamic experiments can help in selecting an appropriate adsorbent material and generating accurate and reliable process simulations [13]. In particular, breakthrough experiments can be used to extract both equilibrium and kinetic information about the adsorbate-adsorbent pair's behavior, such as CO_2/CH_4 adsorption capacities at equilibrium and selectivity, breakpoint times and adsorption capacity at various times during a dynamic test. An effective PSA process engineering starts with the selection of the adsorbent material and includes the definition of adsorption time and designing a regeneration protocol for the adsorbent that consumes the least amount of energy (to lower the associated energetic penalty) and can be completed in the shortest amount of time (to increase productivity) [14]. Nevertheless, due to the complexity of the PSA process' design and implementation, these studies often rely on mathematical models or simulation software rather than specific experimental studies [15–17]. Indeed, the literature on the dynamic performance of adsorbent beds for CO_2/CH_4 separation is limited [18]. Punpee et al. [19] claim that understanding the characteristics of CO_2 adsorption and desorption on the adsorbent material is essential for the application of biogas upgrading. However, this study utilized mathematical models and simulation software instead of experimental investigations. Detailed binary data is crucial for validating models describing PSA performances. For this reason, Álvarez-Gutiérrez and co-workers [20] studied biogas upgrading utilizing a single-column PSA unit, focusing on the dynamic behavior of three adsorbent materials (CS-CO2, CS-H2O and Calgon BPL) in CO_2/CH_4 separation. In this study, it is shown that the separation performance of the adsorbent material is strongly influenced by the adsorption pressure. As the adsorption pressure increases, the CO_2 working capacity increases; however, at 10 bar the CO_2/CH_4 separation efficiency decreases dramatically for all the three adsorbents studied [20]. Using Aspen software, Abd et al. [21] developed a one-dimensional binary mixture model for CO_2 adsorption, energy, and mass transfer, finding good agreement between simulated and experimental data from breakthrough curves conducted for the simulated 45% CO_2/55% CH_4 biogas mixture at 4 bar. Möller et al. [22] investigated the performance of three commercial adsorbent materials in CH_4/CO_2 separation, concluding that simple models based on pure component equilibrium data are unreliable for predicting realistic conditions, and that dynamic experiments are essential for an accurate assessment of fixed-bed behavior. The latter study emphasizes the significance of binary (CO_2/CH_4) dynamic tests, pointing out that a preliminary evaluation of single-compound performances and a fair comparison with retrieved binary data can provide important indications about potential competitive effects and for a thorough use of adsorbent potentiality in the investigated system. The complexity of PSA processes design arises from the numerous variables involved, such as adsorbent material, adsorption pressure, purge ratio and desorption pressure [23]. However, some of these parameters can be defined from a detailed analysis of the chosen adsorbent material. Optimal operating pressure can be determined by considering the adsorbent's adsorption capacity and selectivity (CO_2/CH_4) and the competitive effects can be verified by analyzing the isotherms of pure components and studying the dynamic behavior of the multicomponent system during the adsorption step. The desorption step is critical, involving purging the column with the product flow (CH_4) obtained during the adsorption step. An efficient column regeneration requires optimizing the methane flow rate, with the purge-to-feed ratio (P/F) being pivotal for the process's overall efficiency and effectiveness, especially in biomethane recovery [24]. A high P/F ratio improves methane purity due to a better CO_2 desorption but decreases methane recovery. Achieving high purity and methane recovery, which are generally discordant parameters, necessitates the careful fixing of all the variables [25–29]. Some studies focused on analyzing the adsorbent material to understand the dynamics of CO_2/CH_4 separation during adsorption and, more rarely, desorption. For example, Álvarez-Gutiérrez et al. [30] developed a method for the rapid selection of the most suitable adsorbent material for the PSA operation by comparing the performances in CO_2 separation from biogas of three commercial activated carbons only using CO_2 and CH_4 adsorption data at equilibrium at different pressure (up to 7 bar), but not considering the dynamic behavior of the mixture [30]. With the same objective, Ferella and co-workers [31] compared different synthesized and commercial adsorbent materials by conducting continuous dynamic tests to assess adsorption capacity and CO_2/CH_4 selectivity under relevant industrial conditions. Among commercial adsorbents, in the pressure range from 2 to 6 bar, the material that showed the best selectivity was silica gel, which reported approximately zero methane adsorption at 2 bar, making it a very promising material for CO_2/CH_4 separation with high CH_4 recovery [31]. From the measurement of adsorption isotherms at different temperatures and breakthrough tests, it was shown that an efficient kinetic separation of CH_4 from CO_2 at low pressure can be made with the amino-MIL-53 as the 60%CH_4–40%CO_2 mixture at 1 bar, which exhibits infinite breakthrough selectivity [32]. In the same work, desorption kinetics was studied, calculating the percentages of CO_2 desorbed by purging the adsorbent with He at different temperatures, so to define the optimal time required for desorption [32]. Bacsik et al. [33] compared different adsorbent materials in terms of CO_2 working capacity and selectivity for use in a VSA process, individuating the 4A and 13X zeolites as the most promising ones, thanks to selectivity values above 100. However, the SAPO-56 zeolite, despite having a lower selectivity (20 at 1 bar), has the highest CO_2 working capacity value (2.07 mol kg^{-1} in the 0.1 and 1 bar pressure range), making it a good candidate for the biogas upgrading process [33]. The use of carbon molecular sieves for CO_2/CH_4 separation is scarcely detailed, in term of both adsorption and desorption performances. In a former work [18], we investigated different carbon-based adsorbents, limiting the investigation to atmospheric pressure. Moreover, very few studies in the literature have explored the regenerability of these specific adsorbents during consecutive adsorption-desorption cycles, typical of biogas upgrading with PSA technology [18,19].

This work investigated a commercial carbon molecular sieve, Shirasagi MSC CT-350 (CarboTech), as a selective CO_2 adsorbent in a fixed-bed column-based lab-scale plant. The dynamic adsorption and desorption of CO_2 and CH_4 on the carbon molecular sieve are investigated using breakthrough tests at constant temperature (20 °C) to provide useful information on the material's behavior to be exploited for a

targeted definition of the PSA cycle. Adsorption tests in single-compound systems were conducted at five different pressures of 1, 3, 5, 6.5 and 8 bar to investigate the equilibrium and dynamic fixed-bed behavior, as well as the bed temperature profiles of 40% CO_2/60% He and 60% CH_4/40% He mixtures, with a constant feed flow rate of 2.5 NL/min. To further understand the separation behavior of CH_4 from CO_2, a breakthrough test was conducted using a 40% CO_2/60% CH_4 mixture at an adsorption pressure of 3 bar, under the same partial pressure conditions as the single-compound tests.

Desorption tests were performed to investigate the effect of the purge methane flow rate on bed regeneration time, with variable P/F ratios of 50%, 30%, and 20%, as well as the effect of using a vacuum pump. Finally, the optimal times of the single phases constituting the PSA steps were defined.

2. Materials and methods

2.1. Materials

The adsorbent selected is the commercial carbon molecular sieve (CMS) Shirasagi MSC CT-350, provided by CarboTech (Germany), and commonly applied for CO_2-removal from gas mixtures such as biogas. The main textural properties of the investigated adsorbent are listed in Table 1 [18]. Pure CO_2, CH_4 and Helium tanks gas were supplied by SOL S.P.A. (Italy).

1.1 Lab-scale plant description

The experimental campaign was conducted in a laboratory-scale plant provided by Amnis Pura Ltd. A simplified scheme of the unit is reported in Fig. 1. The plant used for adsorption/desorption experiments consists of one cylindrical stainless-steel column with a height of 440 mm and a diameter of 32 mm. The column is equipped with a thermal jacket, connected to a circulating thermostatic bath, and a thermocouple (TI) inserted in the adsorbent bed, to monitor its temperature. Four solenoid valves (V1 to V4) are associated with the column, which can be set in open or closed position depending on the specific operation to be performed. The adsorption step is conducted by opening valves V1 and V2, allowing the feed to flow into the column from the bottom. In contrast, the desorption step is conducted by opening valves V3 and V4, feeding the column from the top in a countercurrent direction to the adsorption step. In addition, a vacuum pump (Vacuumbrand MZ 2 NT) allows the column to be regenerated at sub-atmospheric pressures. The feed current can be simulated using three mass flow controllers (MFCs) for helium, methane, and carbon dioxide. Moreover, a mass flow meter (MFM) is put at the outlet of the adsorption column to measure the output gas flow. To control the column pressure at the desired level a Pressure Controller (PC) linked to a proportional valve is used, while a Pressure Transmitter (PT) is located at the top of the column for pressure reading and monitoring. The communication between the PC and the MFCs for remote management is run with the programmable logic controller (PLC) through a graphic Excel interface. The gas streams flowing out of the adsorption column were analyzed using a gas analyzer NDIR AO2020 Uras 26 (non-dispersive infrared) model, interfaced to the PC by LabVIEW software.

Table 1
MSC CT-350 microstructural properties.

Geometry	Cylindrical
Average particle diameter [mm]	1.8
Average particle length [mm]	2.5
Bulk density [kg m^{-3}]	705
BET surface area [m^2 g^{-1}]	400
Average pore diameter [nm]	0.4
Ultramicropore volume [cm^3 g^{-1}]	0.22 ± 0.01
Micropore volume [cm^3 g^{-1}]	0.18
Total pore volume [cm^3 g^{-1}]	0.20

2.2. Experimental protocols

A set-up of the experimental apparatus is required to ensure the quality and reliability of the results obtained. A fundamental step in the protocol is instrument calibration. The mass flow controllers (MFC) and the mass flow meter (MFM) were calibrated to account for the actual experimental conditions in the laboratory device. While each MFCs can be calibrated for their respective pure gas, the MFM operates with flows of variable composition, hence its lecture changes. Therefore, the MFM was calibrated at different gas compositions to match the output flow rate read by the MFM and the actual flow rate.

All the experiments were conducted in the previously described single fixed-bed column, packed with 75 g of adsorbent material, achieving a bed height of 15 cm with a bed porosity of 0.37. The rest of the column volume was filled with glass pellets, with an average diameter similar to that of the adsorbent, to minimise the dead volume of the measurement system, and simultaneously minimise the impact on fluid dynamic characteristics of the gas flow.

Before the start of the experimental campaign, the adsorbent material was subjected to heat treatment at 100 °C overnight.

2.3. Breakthrough tests

Experimental tests were conducted with either 40% CO_2/60% He or 60% CH_4/40% He gas mixtures with a constant flow rate of 2.5 NL min^{-1} to fully understand the single-compound adsorption behavior of the CMS. In fact, Helium can be considered a bare gas carrier, as it ideally does not adsorb onto the adsorbent material [34,35]. These tests were conducted at five different adsorption pressures of 1, 3, 5, 6.5 and 8 bar to investigate the effect on adsorption capacities and selectivity. Following that, a breakthrough test was performed using a 60% CO_2/40% CH_4 mixture to simulate a typical biogas composition, with a total flow rate of 2.5 NL min^{-1} and total pressure of 3 bar, to have the same partial pressure conditions to compare with the pure components tests.

The breakthrough experimental runs involved the initial pressurization of the fixed-bed column with He, reaching the desired pressure value. Following the pressurization, the gas mixture containing CO_2 and/or CH_4 was fed into the system. The data of all the gas composition at the outlet of the adsorber, its flow rate and the temperature of the adsorbent bed were recorded.

During the adsorption step, the response at the column exit was monitored until saturation conditions were reached (the bed temperature returning to the initial value, the mole fraction of the adsorbate in the outlet gas becoming equal to the inlet fraction, and the total outlet flow becoming equal to the inlet flow). In particular, the saturation condition specifically refers to the condition in which the adsorbate reaches the thermodynamic equilibrium in the gas and adsorbed phases.

From these breakthrough experiments, the temporal evolution of the partial CO_2 and CH_4 flowrates exiting the column was determined (breakthrough curves), which can be obtained by appropriately matching the volumetric concentrations (% vol.) data at the column outlet ($c_i^{OUT}(t)$), provided by the NDIR analyzer, with the total outlet flowrate data, provided by the MFM (Q_{TOT}^{OUT}).

Moreover, from the same tests, important thermodynamic information can be retrieved. By applying a mass balance equation on the single adsorbed species in the fixed-bed and correcting for the corresponding dead times, dynamic tests were used to obtain the CO_2 and CH_4 equilibrium adsorption capacities, ω_i^{eq} [mol kg^{-1}] (i = CO_2, CH_4). The dead volume of the column increases the residence time of a breakthrough

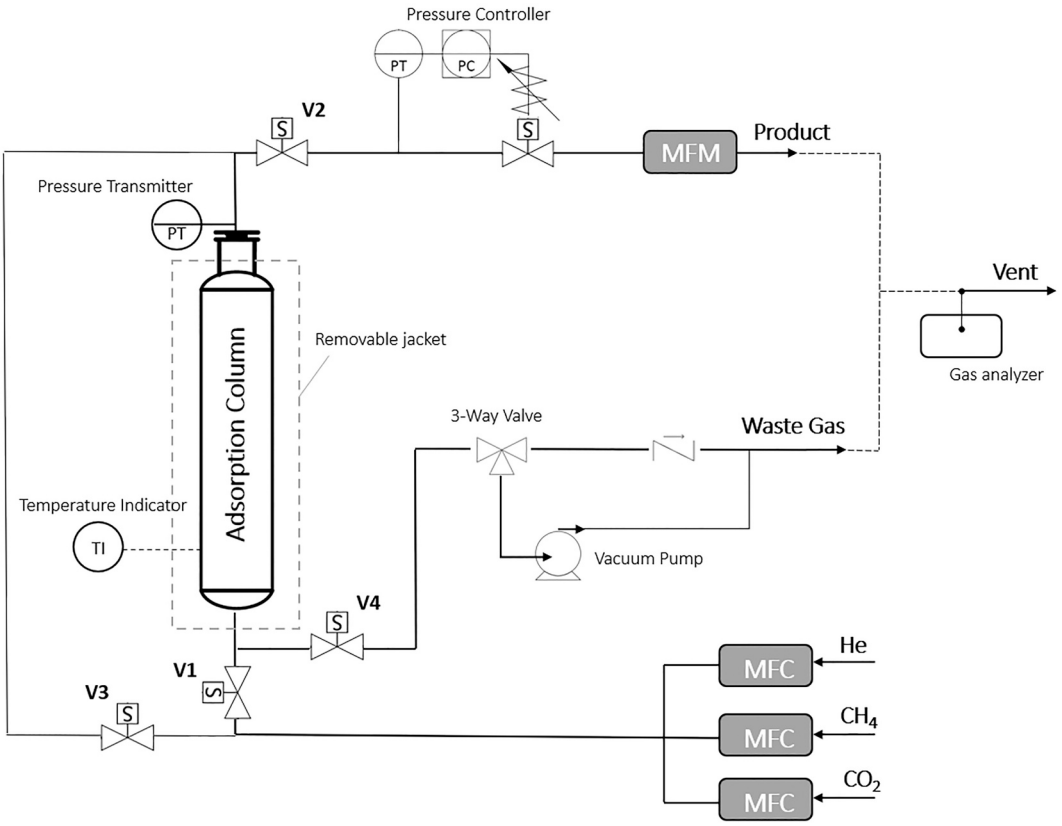

Fig. 1. Simplified schematic diagram of experimental apparatus.

response and leads to an overestimation of the equilibrium capacity based on the uncorrected column breakthrough response. The dead time, which measures the time interval between the start of the test, the exit of the gas from column and the analyzer detection, rises as the column pressurization level does, due to the increase in the amount of gas used for pre-pressurization. To obtain the proper response of the breakthrough column, which can be subsequently analyzed to obtain accurate equilibrium and kinetic data, the measured breakthrough responses must first be corrected from the blank response. The experiment's blank test response was determined by feeding the gas through the adsorption column filled with inert glass beads at the same flow rate, concentration, pressure, and temperature as the breakthrough experiment.

The Equation defined to calculate the correct adsorption capacity, derived from a mass balance on the column, is then as follows:

$$\omega_i^{eq} = \frac{Q_i^{IN}\rho_i}{m}\left[\int_0^{t_s}\left(1-\frac{Q_i^{OUT}(t)}{Q_i^{IN}}\right)dt - \tau_{ads}\right] \quad (1)$$

where:

- Q_i^{IN} [L s^{-1}] is the input volumetric rate of the i-th gas (i = CO_2 or CH_4) (calculated 20 °C and 1 atm);
- ρ_i [mol L^{-1}] is the molar density of the i-th gas at the operating temperature and pressure;
- m [kg] is the mass of the adsorbent;
- Q_i^{OUT} [L s^{-1}] is the output volumetric rate of the i-th gas, obtained from the product of the volumetric fraction of the adsorbate in the outlet flowrate $c_i^{OUT}(t)$ [% vol.] and the total outlet flowrate $Q_{TOT}^{OUT}(t)$ [L s^{-1}], as determined by MFM.
- t_s [s] is the saturation time;
- τ_{ads} [s] is the dead time, defined as the time necessary for the CO_2 (or CH_4) molecules fed as 40% CO_2/60% He (or 60% CH_4/40% He) gas mixtures to a previously He-pressurized bed, filled of inert material (blank test), to arrive to the analyzer and be detected, expressed as:

$$\tau_{ads} = \int_0^{t_s^*}\left(1-\frac{Q_i^{*OUT}(t)}{Q_i^{*IN}}\right)dt \quad (2)$$

where:

- Q_i^{*IN} [L s^{-1}] is the input volumetric rate of the i-th gas of the blank test;
- Q_i^{*OUT} [L s^{-1}] is the output volumetric rate of the i-th gas of the blank test,
- t_s^* [s] is the time for which the molecules fed in the inert column reach the analyzer and be detected.

The mass balance can be also employed to evaluate the adsorption capacity up to a specific time, by replacing the upper bound of the integral (Eq.(1)). This is especially useful for calculating the breakpoint adsorption capacity (ω_i^{BP}), which is the amount of gas captured up to the breakpoint time (t_{BP}), i.e. the time for which c_i^{OUT} reaches the maximum allowable values (e.g. 3% *v/v* for CO_2 in biomethane). This characteristic time is particularly relevant for industrial applications since the adsorption process is stopped at t_{BP} for the target adsorbate to ensure that the output flow gas quality requirements are preserved.

Breakthrough tests at different partial pressure were employed for the evaluation of single-compound adsorption isotherms on the studied adsorbent material.

The selectivity of the adsorbent for CO_2 with respect to CH_4 was evaluated by the following equation [8,17,18]:

$$S_{CO_2/CH_4} = \frac{\omega_{CO_2}^{eq}/c_{CO_2}^{IN}}{\omega_{CH_4}^{eq}/c_{CH_4}^{IN}} \quad (3)$$

Eq. (3) estimates the "Pure Component Selectivity CO_2/CH_4" which is calculated using the equilibrium adsorption capacity defined by a single-compound adsorption test to get an initial selectivity estimate to compare later with binary tests. Using the relative equilibrium adsorption capacity defined by the binary adsorption test, the same Eq. (3) was used to calculate the CO_2/CH_4 selectivity for the binary system.

2.4. Desorption tests

In order to design a PSA cycle, countercurrent desorption tests were conducted to examine the effectiveness of using methane as a purging agent to remove CO_2 during the regeneration phase of the adsorbent bed. Adsorption steps up to the CO_2 t_{BP} were followed by CO_2 desorption steps in the tests. Desorption tests were performed at P/F ratios of 50%, 30%, and 20%, either at atmospheric pressure or under vacuum (using the vacuum pump), to investigate the effect of methane flow rate on adsorbent bed regeneration time.

The adsorption steps up to t_{BP} were carried out at 3 bars with a flow rate of 2.5 NL min^{-1} of the 40% CO_2/60% CH_4 gas mixture. Following atmospheric pressure venting, CO_2 desorption experiments were performed by fluxing pure CH_4 as a desorbing agent and monitoring the CO_2 outlet concentration with an NDIR analyzer until a complete regeneration.

The desorption profiles were elaborated to obtain the total specific amount of CO_2 desorbed from the carbon molecular sieve, $\omega_{CO_2}^{des}$ [mol kg^{-1}], through a material balance. The time for complete desorption ($t_{0.1}$) was assumed as the time in which CO_2 outflow concentration is equal to the analyzer's low detection limit (i.e., 0.1% CO_2 by vol.). The following mass balance on CO_2 over the column can be used to derive the volumetric output flows ($Q_{CO_2}^{OUT}$ [L s^{-1}]) using the output concentration data retrieved from the gas analyzer:

$$Q_{CO_2}^{OUT}(t) = \frac{Q_{CH_4}^{des}(t) c_{CO_2}^{OUT}(t)}{1 - c_{CO_2}^{OUT}(t)} \tag{4}$$

To confirm the same data obtained by adsorption up to BP time, it is possible to calculate the BP adsorption capacity from desorption $\omega_{CO_2}^{des}$ by integrating the volumetric output gas flow across the total desorption time $t_{0.1}$ [s]:

$$\omega_{CO_2}^{des} = \frac{\rho_{CO_2}}{m}\left[\int_0^{t_{0.1}} Q_{CO_2}^{OUT}(t)\, dt - \tau_{des}\right] \tag{5}$$

where:

- τ_{des} [s] is the dead time, defined as the time required for the methane flow rate to replace the CO_2 molecules contained in the column voids. This time is determined by a blank test that was performed in the glass bead-filled column at the same flow rate, pressure, and temperature as the actual experiment, and expressed as:

$$\tau_{des} = \int_0^{t_{0.1}^*} Q_{CO_2}^{*OUT}(t)\, dt \tag{6}$$

By varying the integration interval in Eq. (5), it is possible to determine when a specific amount of adsorbed CO_2 is desorbed.

Because the adsorbents were fully regenerated between tests, the repeatability of breakthrough curves could be evaluated for six consecutive cycles.

3. Results and discussion

3.1. Breakthrough tests in single-component systems

Figs. 2(a) and 3(a) show the dynamic behaviors of outlet CO_2 and CH_4 concentrations obtained from breakthrough tests conducted with CO_2/He and CH_4/He mixtures at total variable pressure, respectively. The breakthrough curves are expressed in terms of the ratio of the volumetric flow rates of the component at the bed outlet relative to that in the feed $Q_i^{OUT}(t)/Q_i^{IN}(t)$. Figs. 2(b) and 3(b) show the temperature profiles inside the adsorbent bed, normalized for the initial test temperature $T(t)/T_{IN}(t)$ from the dynamic experiments conducted for CO_2/He and CH_4/He mixtures, respectively.

The t_{BP} are taken at a volumetric concentration of the adsorbate in the outlet flowrate $c_i^{OUT}(t)$ [% vol.] equal to 3%. It can be observed that methane has an almost instantaneous breakpoint for any value of adsorption pressure, which is a maximum of 5 s at 8 bar. This result is correlated with the low adsorption capacity and also indicates the slow adsorption of CH_4 on the adsorbent. On the contrary, for CO_2, a significant adsorption magnitude can be observed as indicated by far higher breakpoint times, which for pressures of 1, 3, 5, 6.5 and 8 bar equal 50, 120, 170, 200 and 230 s, respectively. As a further confirmation, the temperature profiles of the CO_2 single-compound tests showed a single peak, with a temperature increase proportional to the amount of CO_2 adsorbed as the pressure increased. On the contrary, a flat temperature profile was observed for CH_4, in line with the low adsorption capacity and slow adsorption kinetics. These results are consistent with those retrieved by Cavenati et al. [27] using a 55% CH_4–45% CO_2 mixture on CMS 3K, which emphasized that the temperature rise from CO_2

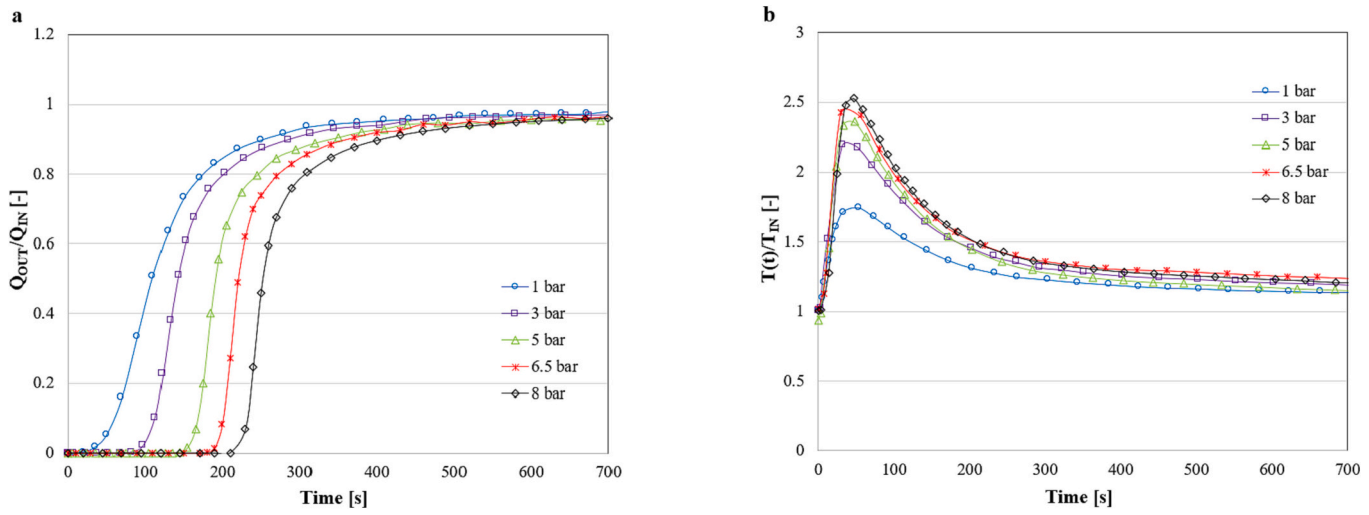

Fig. 2. Experimental a) breakthrough curves and b) temperature profiles along the adsorber column of 40% CO_2/60% He gas mixture on MSC CT-350 at 1, 3, 5, 6.5, 8 bar and 20 °C, feed flow rate 2.5 NL min^{-1}.

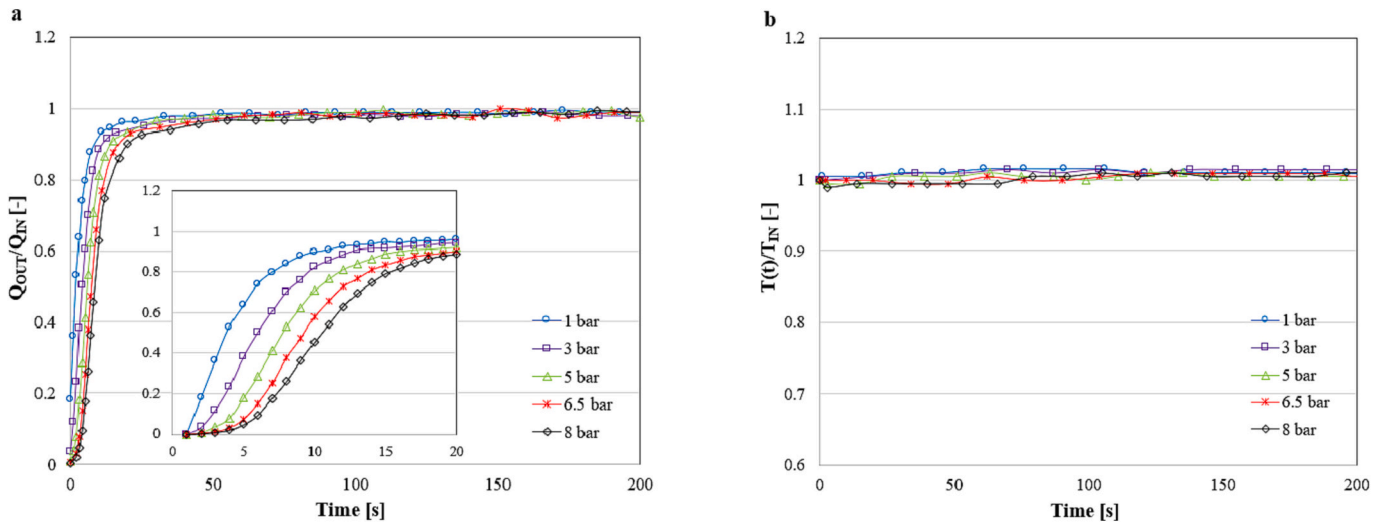

Fig. 3. Experimental a) breakthrough curves and b) temperature profiles along the adsorber column of 60% CH_4/40% He gas mixture on MSC CT-350 at 1, 3, 5, 6.5, 8 bar and 20 °C, feed flow rate 2.5 NL min^{-1}.

adsorption is significant (over 20 °C) and cannot be ignored, whereas the rise from methane adsorption is minimal, showing that the speed of the thermal wave aligns more with the CO_2 concentration wave than with methane's. Indeed, the magnitude of the temperature increase in the profile can be directly correlated with the number of molecules adsorbed over time onto the surface of the adsorbent material. As the partial pressure of CO_2 increases, so does the number of molecules adsorbed, causing a corresponding increase in the temperature peak (Fig. 2b). However, in the case of methane, the number of molecules adsorbed is significantly lower, resulting in a minimal impact on the bed temperature (Fig. 3b). Besides the quantity, another aspect that could affect the magnitude of the temperature increase is the adsorption rate relative to the current feed rate. Suppose the adsorption kinetics is slow relative to the feed rate; in that case, the released adsorption heat is carried away by the gas flow, resulting in a flat temperature profile, as in the case of methane. The shape of the breakthrough curve is affected by pressure, and this is particularly evident for CO_2 breakthrough curves, which have a steeper slope as the pressure increases. The mass-transfer zone (between the breakpoint and saturation), where most of the change in gas concentration occurs, for CO_2 decreases with increasing pressure, resulting in more efficient use of the adsorbent bed. In fact, the mass transfer zone, which depends on both the mass transfer resistance and the shape of the adsorption isotherm [20], affects the bed utilization efficiency expressed as utilized bed fraction, F_{USB}, and defined as the ratio of the adsorption capacity of the adsorbent material at breakpoint ω_i^{BP} to the adsorption capacity at equilibrium ω_i^{eq}. Table 2 shows the F_{USB} for both CO_2 and CH_4 as a function of pressure. For CO_2, a significant increase can be observed, ascribable to the increase in the driving force. On the other hand, for CH_4, the MTZ almost keeps constant, as testified by slight and non-monotonous variations in the F_{USB} values as pressure increases.

The equilibrium adsorption isotherms, as derived from CO_2/He and CH_4/He breakthrough tests at 20 °C for the MSC CT-350 are plotted in Fig. 4, while Table 3 summarizes the equilibrium adsorption capacity of pure CO_2 and pure CH_4 calculated from the breakthrough experiments.

Table 2
Ratio between ω_i^{BP} and ω_i^{eq} (F_{USB}) for CO_2 and CH_4 as a function of pressure.

Total Pressure [bar]	$\omega_{CO_2}^{BP}/\omega_{CO_2}^{eq}$ [−]	$\omega_{CH_4}^{BP}/\omega_{CH_4}^{eq}$ [−]
1	0.25	0.084
3	0.51	0.049
5	0.57	0.050
6.5	0.62	0.072
8	0.70	0.071

The uptakes obtained from the breakthrough experiments indicate that, as expected, both CO_2 and CH_4 adsorption capacity increase along with pressure, and CH_4 adsorption capacities are considerably lower when compared with the corresponding values of CO_2, although retrieved at higher partial pressure (60% vs. 40%). For instance, the CO_2 adsorption capacity at 20 °C increased from 1.39 to 2.87 mol kg^{-1} as the partial pressure increased from 0.4 to 3.2 bar, while for CH_4, the adsorption capacity increased from 0.147 to 0.375 mol kg^{-1} as the partial pressure increased from 0.6 to 4.8 bar. Comparing the values obtained with those retrievable in the literature, for the separation of CO_2 from CH_4 at pressures exceeding atmospheric, equilibrium data for the MSC CT-350 are quite rare. Only one point for CO_2 and methane at partial pressures of 0.4 and 0.6 bar, respectively, could be compared with the data provided by Rainone et al. [18] using the same measuring technique, which resulted in perfect agreement. The CO_2 adsorption isotherm at 20 °C also showed good agreement with the data provided by Möller et al. [36], despite using a different gravimetric measurement technique. On the other hand, the methane adsorption isotherm is only mentioned for temperatures above 40 °C because of the methane's extremely slow adsorption rate. However, CH_4's larger adsorption capacities than those retrieved in the present work were obtained by Song et al. [37] for three commercial CMS, determined by gravimetric analysis, while the values for CO_2 adsorption resulted in the same order of magnitude as the present work. A CO_2 adsorption capacity from 0.50 to 1.80 mol kg^{-1} at 25 °C and partial pressure from 0.5 to 3 bar was found for the CMS that most closely matched the properties of the material under investigation in terms of BET surface area, total pore volume, and micropores; in comparison, a CH_4 adsorption capacity from 0.30 to 1.50 mol kg^{-1} at 25 °C and partial pressure from 0.5 to 5 bar was found [37]. The same finding was obtained when comparing CMS CT-350 with commercial CMS KP-407, for which Rocha et al. [38] verified a CO_2 adsorption capacity from 0.50 to 2.70 mol kg^{-1} at 25 °C at partial pressure from 0.5 to 3 bar and CH_4 adsorption capacity from 0.40 to 1.75 mol kg^{-1} at 25 °C at partial pressure from 0.5 to 5 bar.

This can be ascribed partially to the different measuring techniques employed and the challenge of analyzing the methane adsorption capacity due to its slow adsorption. Beside, it may also be due to the different pore size characteristics of the investigated materials. According to Song et al. [37], the amounts of CH_4 and CO_2 adsorbed are less dependent on the volume of the mesopores and macropores, which nevertheless play a positive role in gas diffusion within the CMS. The

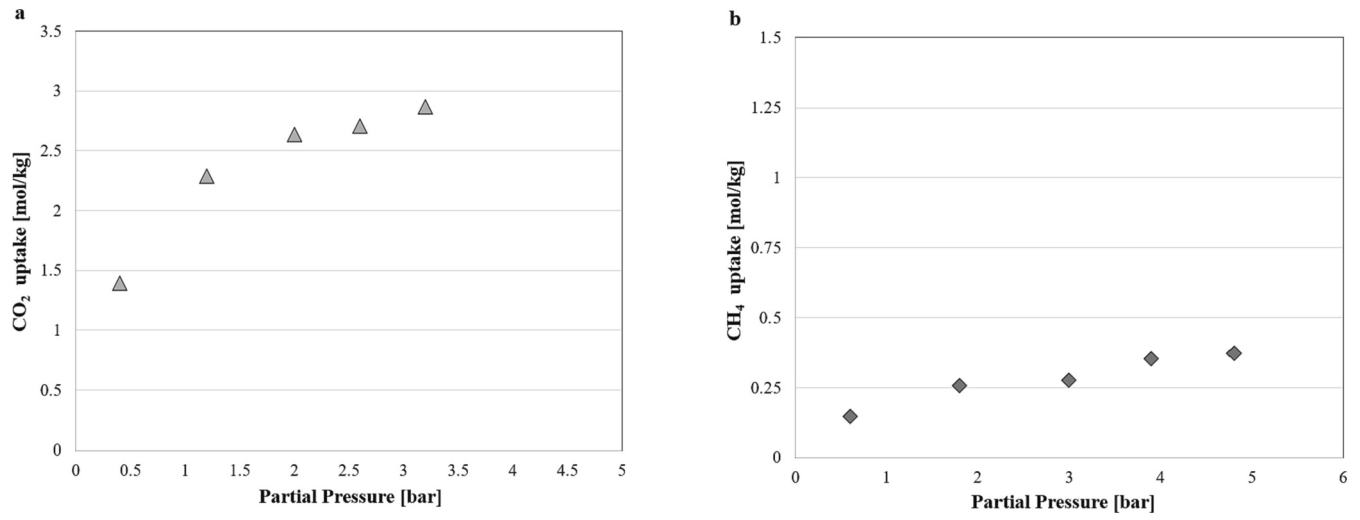

Fig. 4. Adsorption isotherms at 20 °C of a) CO_2 and b) CH_4 on MSC CT-350.

Table 3
CO_2 and CH_4 equilibrium adsorption capacity.

Total Pressure [bar]	CO_2 adsorption capacity [mol kg^{-1}]	CH_4 adsorption capacity [mol kg^{-1}]	Pure Component Selectivity CO_2/CH_4
1	1.39	0.147	14.22
3	2.29	0.262	13.12
5	2.64	0.275	14.40
6.5	2.68	0.354	11.36
8	2.87	0.375	11.48

CMS CT-350 is characterized by a micropore/ultramicropore volume that constitutes 90% of the total pore volume, and this may have contributed to a high adsorption capacity of CO_2 at the expense of the adsorption capacity of CH_4, which also has a larger kinetic diameter than that of CO_2. For these reasons, it is likely to encounter a higher resistance for diffusion into the micropores. These aspects complicate the measurement of methane adsorption capacity even more, which may have led to an underestimation of the values obtained at equilibrium because of the extreme difficulty in achieving a condition of real thermodynamic equilibrium.

A pure component selectivity was calculated from pure component equilibrium adsorption capacity data, as shown in Eq. (3), to get a first estimate of the CO_2/CH_4 selectivity of the molecular sieve. The results indicate that the carbon molecular sieve has a high selectivity toward CO_2. In particular, selectivity shows an almost monotonic evolution, with a decreasing trend from 14.22 to 11.48 for pressure ranging from 1 bar to 8 bar, with slight oscillations likely ascribable to experimental errors in the calculation of methane and CO_2 adsorption capacity values. The obtained selectivities are substantially higher than those reported by Song et al. [37], for CMSs ranging from 1.28 to 1.67 at 10 bar, who calculate the selectivity from single-component isotherms for a 50%/50% CO_2/CH_4 mixture. This could be likely ascribed to the different CMS and to the significantly lower methane adsorption capacity estimates, caused by the mentioned difficulties in measurement due to very slow diffusion in micropores. In agreement with Shen et al. [39], the trend of equilibrium selectivity decreases with increasing pressure; however, at an adsorption pressure of 1 bar and temperature of 30 °C they report an equilibrium selectivity of approximately 2.4. The selectivities reported in the present study are also higher than those retrieved by Álvarez-Gutiérrez et al. [40], with a value of 4.35 on activated carbon (CS-CO_2) and 4.39 on activated carbon (CS-H_2O) for a 50% CO_2 mixture at 303 K and 10 bar. However, the selectivity obtained is lower than the CO_2/N_2 selectivity of 22.84 at 273 K and 1 bar reported by Morali et al. [41], who studied the effects of chemical vapor deposition of methane on activated carbon for the synthesis of CMSs for CO_2 adsorption, emphasizing the importance of a large volume of narrow micropores centered on a size of ca. 0.56 nm to have high CO_2 adsorption capacity and selectivity.

3.2. *Breakthrough test in CO_2/CH_4 binary system*

For a deeper understanding of binary adsorption dynamics, Fig. 5 shows the CH_4 and CO_2 breakthrough curves (a) and temperature profile (b) obtained from the dynamic experiment conducted with the 60% CH_4/40% CO_2 mixture at 3 bar and with a total flow rate of 2.5 NL min^{-1}. A comparison between single-compound and binary tests was conducted to discern any significant differences in adsorption capacity when both components are present, allowing for a more comprehensive understanding of how the presence of two components might influence the separation process. To this aim, the same partial pressures of the mixture components were ensured compared to the partial pressures of the pure components in He.

Fig. 5(a) shows a rapid breakthrough of CH_4, which correlates with both the low adsorption capacity and capture rate of CH_4. This is a desirable result because it reduces the CH_4 loss during adsorption and its content in the off-gas during the regeneration step. Moreover, in the experimental set-up conditions, this effect ensures a time for methane production of up to 2 min. This time corresponds to the difference between the CH_4 and the CO_2 breakpoints. It reveals how effectively the solids bed separates the two adsorbates: the greater the difference in breakpoint times between the two adsorbates, the more efficient is the separation. This breakpoint time difference greatly influences the construction of adsorption/desorption cycles and the related time steps in a PSA process, thus affecting the amount of pure CH_4 produced per cycle.

Concerning the breakpoint times, no significant variations were observed when comparing the test with the corresponding carried out using pure components in helium. For CO_2, a typical sigmoidal breakthrough curve can be observed. On the other hand, a thermal effect, i.e. the partial desorption of CH_4 due to the exothermic adsorption of CO_2, might be responsible for the roll-up on the breakthrough curve of CH_4.

The temperature profile reveals a single peak, and the highest reached value is more than double the initial figure. As stated by Möller et al. [22], the single peak suggests that CO_2, which is not kinetically hindered, is rapidly adsorbed and releases heat, while methane adsorption is extremely low and slow and therefore does not significantly contribute to the temperature rise in the fixed bed, in agreement with the temperature profiles recorded in the single-compound tests. In

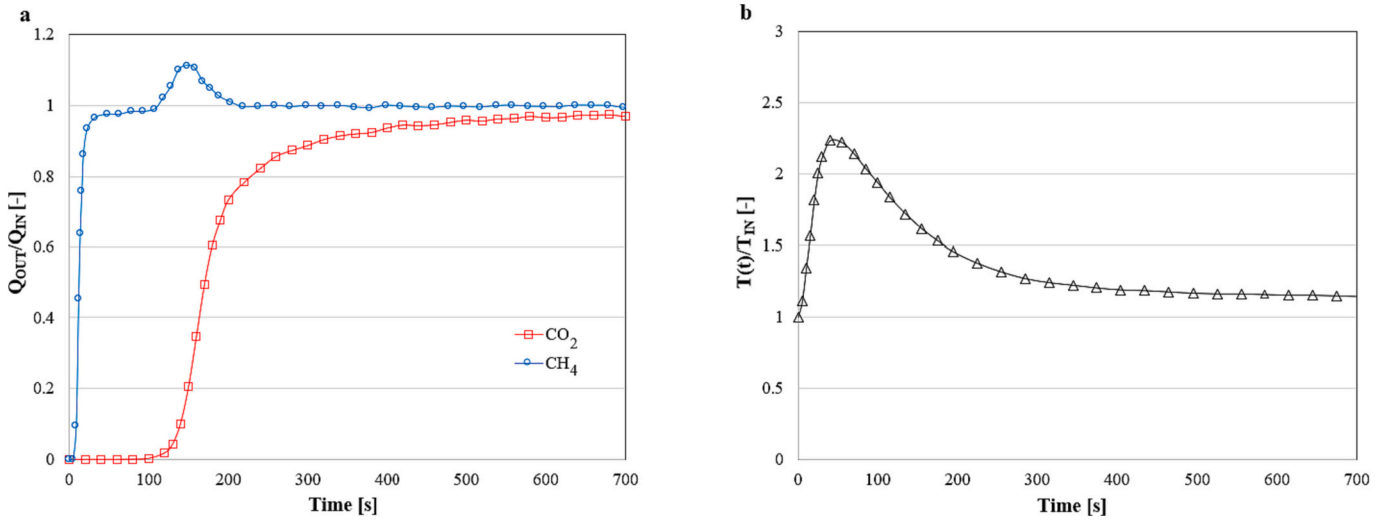

Fig. 5. Experimental a) breakthrough curves and b) temperature profiles along the adsorber column of 40% CO_2 and 60% CH_4 on MSC CT-350 at 3 bar and 20 °C, feed flow rate 2.5 NL min^{-1}.

this case, the experimentally measured adsorption capacity up to the saturation time from the binary mixture's breakthrough curves was 2.16 mol kg^{-1} for CO_2 and 0.302 mol kg^{-1} for CH_4. Compared with the single-compound counterparts, a slight decrease was found in CO_2 adsorption capacity and an equally slight increase in methane's (2.29 mol kg^{-1} for CO_2 and 0.262 mol kg-1 for CH_4). However, these differences appear partly related to experimental uncertainty in the recovered values. For this case, the binary selectivity, calculated as in Eq. (3), is 10.73, lower than the calculation made with the single-component data. In conclusion, it can be stated that a very slight competitive effect between CO_2 and CH_4 can be envisaged.

3.3. Desorption tests

In Fig. 6, the time $t_{i\%}$ [s] required to reach a specified CO_2 recovery percentage of the total adsorbed amount (e.g., $t_{95\%}$ corresponds to 95% of total CO_2 recovered by desorption) is reported as a function of the P/F ratio (flow rate of methane to purge related to the feed) and either with or without the use of the vacuum pump. Without the use of the vacuum pump, the pressure in the column during the desorption step was equal to 1 bar, while with the use of the vacuum pump for P/F of 50%, 30%, and 20%, a pressure of 0.16 bar, 0.11 bar, and 0.08 bar was achieved, respectively.

Table 4 summarizes the desorption times needed to achieve 100%, 95%, 90%, 75% and 50% ($t_{i\%}$ [s]) of the CO_2 adsorbed amount in the adsorption phase until the t_{BP}.

As the purge flow rate used for desorption increases, the time required for a complete regeneration decreases. Moreover, the complete regeneration without the vacuum pump takes between 4300 and 2600 s, while using the vacuum pump the time significantly reduces, taking between 3700 and 1700 s.

Table 4
Desorption time of a percentage of the amount of CO_2 adsorbed, depending on the P/F ratio and the use of vacuum pump.

Pressure [bar]	P/F [%]	$t_{100\%}$ [s]	$t_{95\%}$ [s]	$t_{90\%}$ [s]	$t_{75\%}$ [s]	$t_{50\%}$ [s]
1.00	20	4300	1960	1460	780	310
1.00	30	3700	1800	1300	650	250
1.00	50	2600	1100	700	360	145
0.08	20	3700	900	600	300	125
0.11	30	2100	700	500	250	100
0.16	50	1700	650	470	240	95

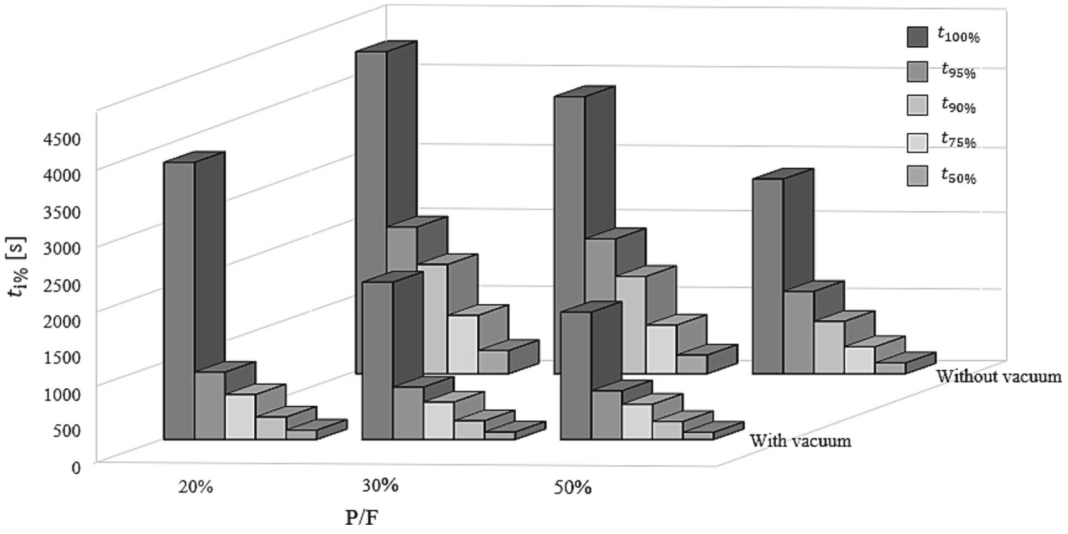

Fig. 6. Time to reach a fixed CO_2 recovery percentage (i.e., $t_{i\%}$ desorption time) as a function of P/F ratio and either with the use of the vacuum pump or without.

In an actual PSA process, the feed step usually ends before the component with the strongest adsorbed force breaks through the bed (hence, the solid is not saturated with CO_2). In contrast, the regeneration step is generally terminated before the bed is fully regenerated because the last part of the regeneration process is usually prolonged and consumes a large amount of purge gas. In light of these observations, times corresponding to lower regeneration rates were also investigated. In particular, without the vacuum pump, a 50% bed regeneration from CO_2 takes between 310 and 145 s, while using the vacuum pump the time reduces significantly, taking between 125 and 95 s. Punpee et al. [19], from desorption curves simulated with Aspen Adsorption for three adsorbent materials, estimated that after 40 s the amount of CO_2 desorbed with the vacuum pump at 0.1 bar was 18%, 43% and 37% for zeolite, CMS and AC, respectively.

In general, due to a slow kinetics, the time for a complete regeneration ($t_{100\%}$) of the adsorbent is very long. In addition, during desorption, most of the adsorbed CO_2 is rapidly removed, but subsequently the rate of desorption decreases significantly over time. For instance, for the desorption of 95% of the amount of CO_2 adsorbed, a reduction in desorption time $>$ 50%, compared to the figure needed for a complete regeneration, is retrieved. This is due to the peculiar characteristics of the adsorbent material, most of whose total volume consists of micropores. This, on the one hand allows strong CO_2 adsorption capacity and selectivity, but on the other hand makes regeneration of the material very hard. In fact, to have desorption step times comparable with adsorption step times very low vacuum pressure and high purge flow rates are required.

As can be observed, a higher purge flow rate results in a shorter desorption time. However, it is also essential to consider the total amount of methane required during the desorption process. During a hypothetical PSA cycle, the amount of methane employed for desorption significantly impacts the slip of methane in the off-gas stream, making it a crucial factor to evaluate. The results show that, on average, as the purge flow rate increases, so does the amount of methane consumed for desorption. For instance, with a 90% regeneration rate and using the vacuum pump, the total amount of methane consumed for a P/F ratio of 50%, 30%, and 20% is 10 L, 6 L and 5 L, respectively. Therefore, a balance between minimizing the methane losses and achieving an acceptable desorption degree in a reasonable desorption time is essential.

3.4. Adsorption-desorption cyclic tests

Finally, to evaluate the regenerative capability of the CMS, CO_2 adsorption and desorption tests were carried out in consecutive cycles. In the column, the adsorption step was conducted at 3 bar with the 40% CO_2/60% CH_4 (vol.) mixture of 2.5 NL/min for a time equal to the breakpoint time of CO_2 at 3 bar (120 s), and the desorption step was conducted until complete regeneration of the adsorbent with a P/F ratio of 50% and pressure of 0.16 bar (1700 s), alternated sequentially. The aim was to determine if the adsorbent could be reused after regeneration, and to assess any potential loss of CO_2 adsorption capacity due to an iterative use. The experimental results in Fig. 7 indicate that the $\omega_{CO_2}^{BP}$ remains consistently stable across the number of cycles, with minimal variations likely attributed to experimental uncertainty. In details, the CO_2 adsorption capacity of MSC CT-350 remained almost constant at 1.07 mol kg^{-1} throughout all consecutive adsorption/desorption cycles. This suggests that adsorption is reversible, confirming the complete regenerability of the adsorbent.

4. Conclusions

Carbon molecular sieves can be proficiently used in processes to separate CO_2 from CH_4, such as in PSA technology for upgrading biogas to biomethane. However, only some studies base the design of separation processes on the specific characteristics of such sorbents. To provide essential data for the design of a PSA process, the carbon molecular sieve MCS CT-350 was experimentally evaluated for the dynamic adsorption and desorption of CO_2 and CH_4. The main results are listed below:

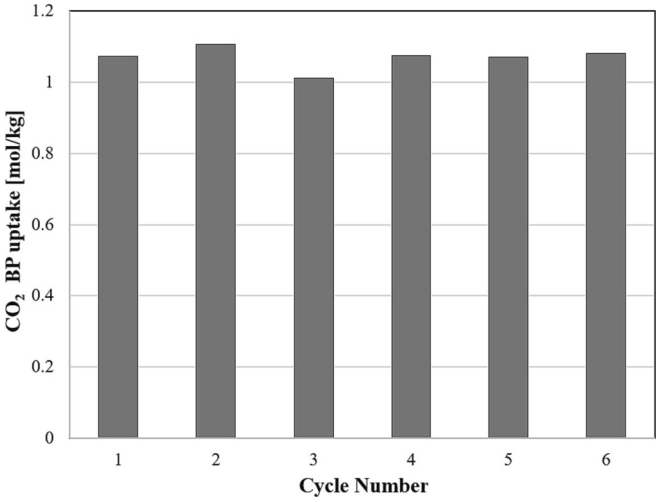

Fig. 7. CO_2 adsorption capacity of the MSC CT-350 at breakpoint time over consecutive adsorption/desorption cycles of a 40% CO_2/60% CH_4 (vol.) mixture. $P = 3$ bar; $T = 20$ °C.

1) In single-compound systems, methane showed an instantaneous breakpoint of a maximum of 5 s at 8 bar, indicating the low magnitude and slow kinetics of CH_4 adsorption on the adsorbent bed, consistent with the retrieved isothermal temperature profile. On the contrary, CO_2 showed an increasing breakpoint time with pressure, ranging from 50 s to 230 s at 1 to 8 bar pressures.
2) CO_2 has a significantly higher adsorption capacity at equilibrium than CH_4. The figures obtained for different pressures and constant temperature of 20 °C for CO_2 increased from 1.39 to 2.87 mol kg^{-1}, while for CH_4 increased from 0.147 to 0.375 mol kg^{-1}.
3) From a dynamic experiment conducted with a 60% CH_4/40% CO_2 mixture to better understand the binary adsorption dynamics, no significant differences were observed in terms of both equilibrium and kinetic properties with respect to pure compounds data.
4) Desorption tests purging methane after CO_2/CH_4 adsorption revealed that as the P/F ratio increases, the time required for regeneration decreases, and this time is significantly reduced with the use of the vacuum pump. Full regeneration times ranged from 4300 s to 1700 s, but partial regeneration at 95% adsorbed amount showed $>$ 50% reduction, ranging from 1460 s to 470 s.
5) Finally, it was shown that the adsorbent is regenerable and may be used repeatedly in subsequent adsorption-desorption cycles at breakpoint without significantly losing its ability to absorb CO_2.

In conclusion, the high CO_2 adsorption capacity of MSC CT-350 as compared to CH_4, and the excellent regeneration capabilities confirmed the applicability to CO_2/CH_4 separation processes. Furthermore, the adsorption and desorption kinetics results provide valuable indications for designing a PSA process, particularly for defining the time required for the adsorption and desorption steps.

Funding sources

This work was supported by Regione Lombardia (Italy) under the Program “Programmi Operativi Regionali finanziati con Fondo Europeo di Sviluppo Regionale 2014–2020”.

CRediT authorship contribution statement

Esther Pancione: Writing – original draft, Validation, Software, Investigation, Data curation, Conceptualization. **Francesco La Motta:** Writing – review & editing, Validation, Supervision, Resources, Project administration, Funding acquisition, Formal analysis. **Amedeo Lancia:** Writing – review & editing, Validation, Supervision, Formal analysis. **Alessandro Erto:** Conceptualization, Writing – review & editing, Formal analysis, Supervision, Validation, Resources, Funding acquisition.

Declaration of competing interest

The authors declare that they have no known competing financial interests or personal relationships that could have appeared to influence the work reported in this paper.

Data availability

Data will be made available on request.

Acknowledgments

The authors would like to thank the Regione Lombardia (Italy) for support in the process of designing the experimental apparatus and procedure under the Program "Programmi Operativi Regionali finanziati con Fondo Europeo di Sviluppo Regionale 2014-2020", in relation to "Asse I – Rafforzare la ricerca lo sviluppo e l'innovazione, Azione I.1. b.1.1 - Sostegno all'acquisto di servizi per l'innovazione tecnologica strategica organizzativa e commerciale delle imprese".

References

[1] M. Balsamo, F. Montagnaro, E.J. Anthony, Socio-economic parameters affect CO_2 emissions and energy consumption – an analysis over the United Nations Countries, Curr. Opin. Green Sustain. Chem. 40 (2023) 100740, https://doi.org/10.1016/j.cogsc.2022.100740.

[2] A. Golmakani, S.A. Nabavi, B. Wadi, V. Manovic, Advances, challenges, and perspectives of biogas cleaning, upgrading, and utilisation, Fuel 317 (2022) 123085, https://doi.org/10.1016/j.fuel.2021.123085.

[3] European Commission, Renewable energy Directive EU/2023/2413. https://energy.ec.europa.eu/topics/renewable-energy/renewable-energy-directive-targets-and-rules/renewable-energy-directive_en (accessed 11 December 2023).

[4] EBA, European Biogas Association. "European Biomethane Map 2020". https://www.europeanbiogas.eu/the-european-biomethane-map-2020-shows-a-51-increase-of-biomethane-plants-in-europe-in-two-years/, 2020 (accessed 11 December 2023).

[5] S.S. Hosseini, J.F.M. Denayer, Biogas upgrading by adsorption processes: Mathematical modeling, simulation and optimization approach – a review, J. Environ. Chem. Eng. 10 (2022) 107483, https://doi.org/10.1016/j.jece.2022.107483.

[6] A.A. Abd, M.R. Othman, S.Z. Naji, A.S. Hashim, Methane enrichment in biogas mixture using pressure swing adsorption: process fundamental and design parameters, Materi. Today Sustain. 11-12 (2021) 100063, https://doi.org/10.1016/j.mtsust.2021.100063.

[7] E. Surra, R.P.P.L. Ribeiro, T. Santos, M. Bernardo, J.P.B. Mota, N. Lapa, I.A.A. C. Esteves, Evaluation of activated carbons produced from Maize Cob Waste for Evaluation of activated carbons produced from Maize Cob Waste for, J. Environ. Chem. Eng. 10 (2022) 107065, https://doi.org/10.1016/j.jece.2021.107065.

[8] D.M. Ruthven, S. Farooq, K.S. Knaebel, Pressure Swing Adsorption, VCH, New York, 1994.

[9] D.M. Ruthven, Principles of Adsorption and Adsorption Processes, John Wiley & Sons, New York, 1984.

[10] M.H.V. Bahruna, A. Bono, N. Othman, M.A.A. Zaini, Carbon dioxide removal from biogas through pressure swing adsorption – a review, Chem. Eng. Res. Des. 183 (2022) 285–306, https://doi.org/10.1016/j.cherd.2022.05.012.

[11] R.L.S. Canevesi, K.A. Andreassen, E.A. da Silva, C.E. Borba, C.A. Grande, Pressure swing adsorption for biogas upgrading with carbon molecular sieve, Ind. Eng. Chem. Res. 57 (2018) 8057–8067, https://doi.org/10.1021/acs.iecr.8b00996.

[12] R.L.S. Canevesi, C.E. Borba, E.A. Silva, C.A. Grande, Towards a design of a pressure swing adsorption unit for small scale biogas upgrading at, Energy Procedia 158 (2019) 848–853, https://doi.org/10.1016/j.egypro.2019.01.220.

[13] C.A. Grande, V.M.T.M. Silva, C. Gigola, A.E. Rodrigues, Adsorption of propane and propylene onto carbon molecular sieve, Carbon 41 (2003) 2533–2545, https://doi.org/10.1016/S0008-6223(03)00304-X.

[14] C.A. Grande, Biogas upgrading by pressure swing adsorption, in: Biofuel's Engineering Process Technology, InTech, 2011, https://doi.org/10.5772/18428.

[15] R. Augelletti, M. Conti, M.C. Annesini, Pressure swing adsorption for biogas upgrading. A new process configuration for the separation of biomethane and carbon dioxide, J. Clean. Prod. 140 (2017) 1390–1398, https://doi.org/10.1016/j.jclepro.2016.10.013.

[16] Y.F. Chen, P.W. Lin, W.H. Chen, F.Y. Yen, H.S. Yang, C.T. Chou, Biogas Upgrading by Pressure Swing Adsorption with Design of Experiments, Processes 9 (2021) 1325, https://doi.org/10.3390/pr9081325.

[17] B. Wu, X. Zhang, Y. Xu, D. Bao, S. Zhang, Assessment of the energy consumption of the biogas upgrading process with pressure swing adsorption using novel adsorbents, J. Clean. Prod. 101 (2015) 251–261, https://doi.org/10.1016/j.jclepro.2015.03.082.

[18] F. Rainone, O. D'Agostino, A. Erto, M. Balsamo, A. Lancia, Biogas upgrading by adsorption onto activated carbon and carbon molecular sieves: Experimental and modelling study in binary CO_2/CH_4 mixture, J. Environ. Chem. Eng. 9 (2021) 106256, https://doi.org/10.1016/j.jece.2021.106256.

[19] S. Punpee, P. Tongpadungrod, T. Suttikul, C. Phalakornkule, Characteristics of CO_2 adsorption and desorption on activated carbon in comparison with zeolite 13X and carbon molecular sieve and applications in biogas upgrading using vacuum pressure swing adsorption, J. Chem. Technol. Biotechnol. 98 (2023) 2677–2690, https://doi.org/10.1002/jctb.7320.

[20] N. Álvarez-Gutiérrez, S. García, M.V. Gil, F. Rubiera, C. Pevida, Dynamic Performance of Biomass-based Carbons for CO_2/CH_4 Separation. Approximation to a pressure swing adsorption process for biogas upgrading, Energy Fuel 30 (2016) 5005–5015, https://doi.org/10.1021/acs.energyfuels.6b00664.

[21] A.A. Abd, M.R. Othman, Biogas upgrading to fuel grade methane using pressure swing adsorption: Parametric sensitivity analysis on an industrial scale, Fuel 308 (2022) 121986, https://doi.org/10.1016/j.fuel.2021.121986.

[22] A. Möller, R. Eschrich, C. Reichenbach, J. Guderian, M. Lange, J. Möllmer, Dynamic and equilibrium-based investigations of CO_2-removal from CH_4-rich gas mixtures on microporous adsorbents, Adsorption 23 (2017) 197–209, https://doi.org/10.1007/s10450-016-9821-x.

[23] Y.J. Kim, Y.S. Nam, Y.T. Kang, Study on a numerical model and PSA (pressure swing adsorption) process experiment for CH_4/CO_2 separation from biogas, Energy 91 (2015) 732–741, https://doi.org/10.1016/j.energy.2015.08.086.

[24] G. Shah, E. Ahmad, K.K. Pant, V.K. Vijay, Comprehending the contemporary state of art in biogas enrichment and CO_2 capture technologies via swing adsorption, Int. J. Hydrog. Energy 46 (2021) 6588–6612, https://doi.org/10.1016/j.ijhydene.2020.11.116.

[25] R.L.S. Canevesi, K.A. Andreassen, E.A. da Silva, C.E. Borba, C.A. Grande, Evaluation of simplified pressure swing adsorption cycles for biomethane production, Adsorption 25 (2019) 783–793, https://doi.org/10.1007/s10450-019-00049-x.

[26] J. Shang, A. Hanif, G. Li, G. Xiao, J.Z. Liu, P. Xiao, P.A. Webley, Separation of CO_2 and CH_4 by pressure Swing Adsorption using a Molecular Trapdoor Chabazite Adsorbent for Natural Gas Purification, Ind. Eng. Chem. Res. 59 (2020) 7857–7865, https://doi.org/10.1021/acs.iecr.0c00317.

[27] S. Cavenati, C.A. Grande, A.E. Rodrigues, Upgrade of methane from Landfill Gas by pressure Swing Adsorption, Energy Fuel 19 (2005) 2545–2555, https://doi.org/10.1021/ef050072h.

[28] M.P.S. Santos, A. Carlos, A.E. Rodrigues, Pressure swing adsorption for biogas upgrading, in: Effect of Recycling Streams in Pressure Swing Adsorption Design, Industrial & Engineering Chemistry Research 50, 2011, pp. 974–985, https://doi.org/10.1021/ie100757u.

[29] J. Khunpolgrang, S. Yosantea, A. Kongnoo, C. Phalakornku, Alternative PSA process cycle with combined vacuum regeneration and nitrogen purging for CH_4/CO_2 separation, Fuel 140 (2015) 171–177, https://doi.org/10.1016/j.fuel.2014.09.100.

[30] N. Álvarez-Gutiérrez, M.V. Gil, F. Rubiera, C. Pevida, Simplistic approach for preliminary screening of potential carbon adsorbents for CO_2 separation from biogas, J. CO2 Utilization 28 (2018) 207–215, https://doi.org/10.1016/j.jcou.2018.10.001.

[31] F. Ferella, A. Puca, G. Taglieri, L. Rossi, K. Gallucci, Separation of carbon dioxide for biogas upgrading to biomethane, J. Clean. Prod. 164 (2017) 1205–1218, https://doi.org/10.1016/j.jclepro.2017.07.037.

[32] S.A. Peter, J.F.M. Denayer, G.V. Baron, Kinetic Gas Separation using Small Pore Metal Organic Frameworks, in: Dynamic Desorption and Pressure Swing Adsorption Studies of CO2 and CH4 in Amino-MIL–53 (Al) for Biogas Upgradation, 2013.

[33] Z. Bacsik, O. Cheung, P. Vasiliev, N. Hedin, Selective separation of CO_2 and CH_4 for biogas upgrading on zeolite NaKA and SAPO-56, Appl. Energy 162 (2016) 613–621, https://doi.org/10.1016/j.apenergy.2015.10.109.

[34] T. Saleman, G. Xiao, G. Li, E.F. May, A robust dynamic column breakthrough technique for high pressure measurements of adsorption equilibria and kinetics, Adsorption 23 (2017) 671–684, https://doi.org/10.1007/s10450-017-9884-3.

[35] N.S. Wilkins, A. Rajendran, S. Farooq, Dynamic column breakthrough experiments for measurement of adsorption equilibrium and kinetics, Adsorption 27 (2021) 397–422, https://doi.org/10.1007/s10450-020-00269-6.

[36] A. Möller, J. Guderian, J. Möllmer, M. Lange, J. Hofmann, R. Gläser, Kinetic Separation of methane Containing Gas Mixtures via Carbon Molecular Sieves, Chem. Ing. Tech. 86 (2014) 41–46, https://doi.org/10.1002/cite.201300067.

[37] X. Song, L. Wang, X. Ma, Y. Zeng, Adsorption equilibrium and thermodynamics of CO_2 and CH_4 on carbon molecular sieves, Appl. Surf. Sci. 396 (2017) 870–878, https://doi.org/10.1016/j.apsusc.2016.11.050.

[38] L.A.M. Rocha, K.A. Andreassen, C.A. Grande, Separation of CO_2/CH_4 using carbon molecular sieve (CMS) at low and high pressure, Chem. Eng. Sci. 164 (2017), https://doi.org/10.1016/j.ces.2017.01.071, 148–127.
[39] Z. Shen, Z.Y. Niu, R.Y. Zhang, D. Zhang, Vacuum pressure swing adsorption process with carbon molecular sieve for CO_2 separation from biogas, J. CO2 Utilization 54 (2021) 101764, https://doi.org/10.1016/j.jcou.2021.101764.
[40] N. Álvarez-Gutiérrez, M.V. Gil, F. Rubiera, C. Pevida, Adsorption performance indicators for the CO_2/CH_4 separation: Application to biomass-based activated carbons, Fuel Process. Technol. 142 (2016) 361–369, https://doi.org/10.1016/j.fuproc.2015.10.038.
[41] U. Morali, H. Demiral, S. Sensoz, Synthesis of carbon molecular sieve for carbon dioxide adsorption: Cheical vapor deposition combined with Taguchi design of experiment method, Powder Technol. 355 (2019) 716–726, https://doi.org/10.1016/j.powtec.2019.07.101.